

# Directed Spiral Percolation Hull on the Square and Triangular Lattices

Santanu Sinha and S. B. Santra

*Department of Physics, Indian Institute of Technology*

*Guwahati, Guwahati-781039, Assam, India.*

(Dated: February 2, 2008)

## Abstract

Critical properties of hulls of directed spiral percolation (DSP) clusters are studied on the square and triangular lattices in two dimensions ( $2D$ ). The hull fractal dimension ( $d_H$ ) and some of the critical exponents associated with different moments of the hull size distribution function of the anisotropic DSP clusters are reported here. The values of  $d_H$  and other critical exponents are found the same within error bars on both the lattices. The universality of the hull's critical exponents then holds true between the square and triangular lattices in  $2D$  unlike the cluster's critical exponents which exhibit a breakdown of universality. The hull fractal dimension ( $d_H \approx 1.46$ ) is also found close to  $4/3$  and away from  $7/4$ , that of ordinary percolation cluster hull. A new conjecture is proposed for the hull fractal dimension ( $d_H$ ) in terms of two connectivity length exponents ( $\nu_{\parallel}$  &  $\nu_{\perp}$ ) of the anisotropic clusters generated here. The values of  $d_H$  and other critical exponents obtained here are very close to that of the spiral percolation cluster hull. The hull properties of the DSP clusters are then mostly determined by the rotational constraint and almost independent on the directional constraint present in the model.

## I. INTRODUCTION

Directed spiral percolation (DSP), a new site percolation model, is recently introduced by Santra and Sinha [1, 2]. The DSP model is constructed imposing both directional and rotational constraints on the ordinary percolation model [3]. The directional constraint is in a fixed direction in space and the empty sites in that direction are accessible to occupation. Due to the rotational constraint the sites in the forward direction or in a rotational direction, say clockwise, are accessible to occupation. The direction of the rotational constraint is not fixed in space and it depends on the direction from which the present site is occupied. The cluster properties of the DSP model has already been studied on the square[1] and triangular[2] lattices in two dimensions ( $2D$ ) at their respective percolation thresholds. The DSP clusters were found highly rarefied and anisotropic with chiral dangling ends. It was observed that the values of the critical exponents obtained on both the lattices are different from that of other percolation models like ordinary percolation (OP)[3], directed percolation (DP)[4], and spiral percolation (SP)[5]. The clusters on the triangular lattice were found more compact and less anisotropic than the clusters on the square lattice due to higher number of connectivity on the triangular lattice. It was found that the DSP model not only belongs to a new universality class than other percolation models but also exhibits a breakdown of universality in the cluster properties between the square and triangular lattices in  $2D$ [2].

The hull of a cluster is a continuous path of occupied sites at the external boundary of the cluster. The hull has important significance of its own apart from being a part of the percolation cluster. It has connection with the physical problems like nucleation and growth[6], surface reaction[7], diffusion[8] etc. The hulls also exhibit scaling behaviour, different from that of clusters, characterized by critical exponents at the percolation threshold [9, 10]. Since the clusters generated in the DSP model are anisotropic and chiral in nature, it is interesting to study the critical behaviour of these anisotropic hulls with chiral dangling ends at  $p = p_c$ .

In this paper, the critical properties of hulls of anisotropic DSP clusters are studied on both the square and triangular lattices. Results of anisotropic hull are not reported before and this is the first study of anisotropic-chiral hull properties. A comparison is made between the results obtained on the two lattices as well as in different models, like OP and SP.

## II. CLUSTER GENERATION AND HULL EXTRACTION

A single cluster growth Monte Carlo (MC) algorithm has already been developed in Ref.[1, 2] to generate clusters under the presence of both directional and rotational constraints following the original algorithm of Leath[11]. A brief description of the model is given here. In this algorithm, the central site of the lattice is occupied with unit probability. All the nearest neighbours of the central site can be occupied with equal probability  $p$  in the first time step. As soon as a site is occupied, the direction from which it is occupied is assigned to it. Selection of empty nearest neighbours in the next MC time steps is illustrated for the square lattice in Figure 1(a) and triangular lattice in Figure 1(b). The descriptions given below are valid for both Figure 1(a) and 1(b). Two long arrows from left to right represent the directional constraint. The presence of the rotational constraint is shown by the encircled dots. The black circles represent the occupied sites and the open circles represent the empty sites. The direction from which the central site is occupied is represented by a short thick arrow. The eligible empty site for occupation due to the directional constraint is indicated by the dotted arrow and the thin solid arrows indicate the eligible empty sites for occupation due to the rotational constraint. There are two empty sites due to the rotational constraint eligible for occupation at any MC step on the square lattice, as shown in Figure 1(a), whereas on the triangular lattice there are three such sites available, as shown in Figure 1(b). After selecting the eligible sites for occupation, they are occupied with probability  $p$ . The coordinate of an occupied site in a cluster is denoted by  $(x,y)$ . Periodic boundary conditions are applied in both directions and the coordinates of the occupied sites are adjusted accordingly whenever the boundary is crossed. At each time step the span of the cluster in the  $x$  and  $y$  directions  $L_x = x_{max} - x_{min}$  and  $L_y = y_{max} - y_{min}$  are determined. If  $L_x$  or  $L_y \geq L$ , the system size, then the cluster is considered to be a spanning cluster. The critical percolation probability  $p_c$  is defined as below which there is no spanning cluster and at  $p = p_c$  a spanning cluster appears for the first time in the system.

As soon as a cluster is generated, the hull of the cluster is determined by the method of Ziff *et al* [12]. The hull of a cluster is defined to be the continuous path of occupied sites at the external boundary of the cluster. To determine the hull, a pair of occupied and empty nearest neighbour sites on the external boundary is chosen. An arrow is drawn from the empty site to the occupied site to define a direction and one moves to the occupied

site. Facing to the direction of the arrow, a search is made starting from the left for an occupied nearest neighbour. As soon as an occupied site is encountered an arrow is drawn from the present site to the new occupied site and one moves to the new occupied site. The process is continued until the path passes the starting point in the same direction as it had first been passed. All the occupied sites encountered during this walk are listed in an array called as hull of the cluster. Typical hulls extracted from the clusters generated at the percolation thresholds on the square and triangular lattices are shown in Figure 2 and Figure 3, respectively. It could be seen from the hull itself that the corresponding clusters are more anisotropic on the square lattice than on the triangular lattice. However, both the hulls contain chiral dangling ends and look very similar on small length scales.

### III. SCALING RELATIONS

Analogous to the cluster related quantities, the hull related quantities also exhibit critical properties at the percolation threshold  $p_c$ . The corresponding critical exponents associated to hull related quantities are expected to satisfy certain scaling relations among themselves similar to the scaling relations satisfied by the critical exponents of the cluster related quantities. The scaling theory of the cluster related quantities for the DSP clusters has already been developed in Ref.[1]. In this section, the critical exponents of the analogous hull related quantities will be defined and their scaling relations will be developed. The size of a hull  $H$  is given by the number of occupied sites present on the hull as the size of a cluster  $S$  is given by the number of occupied sites in a cluster. At  $p_c$ , the size of the infinite cluster goes as

$$S_\infty \sim L^{d_f} \quad (1)$$

with the system size  $L$  and  $d_f$  is the fractal dimension of the infinite cluster. The value of  $d_f$  has already been estimated on both the square [1] and triangular [2] lattices. For hulls, a similar relation is assumed here between the size of the largest hull  $H_\infty$  with the system size  $L$  as

$$H_\infty \sim L^{d_H} \quad (2)$$

where  $d_H$  is the hull dimension. The value of  $d_H$  then can be determined measuring  $H_\infty$  for different system sizes  $L$ . It may be noted here that the so-called Ziff's method [13] is not suitable to determine the hull dimension of the anisotropic clusters generated here. In

Ziff's method, the linear distance is measured for a given number of sites along the hull. Since there are two length scales ( $\xi_{\parallel}$  and  $\xi_{\perp}$ ) involved in the DSP clusters, there will be a crossover from  $\xi_{\perp}$  to  $\xi_{\parallel}$  as one measures the linear distance from smaller number of sites to larger number of sites. The average length of a given number of occupied sites will be then strongly dependent on the initial point chosen.

From equations 1 and 2, one can easily verify the relation between the cluster size  $S_{\infty}$  and the corresponding hull size  $H_{\infty}$  for the spanning clusters and it is given by

$$H_{\infty} \sim S_{\infty}^x, \quad x = d_H/d_f \quad (3)$$

where  $d_H$  and  $d_f$  are the fractal dimensions of the hull and the corresponding percolation cluster, respectively. The value of  $d_H$  obtained from equation 2 then could be verified measuring  $x$  and  $d_f$  independently.

The hull size distribution is defined as

$$P_H(p) = N_H/N_{tot} \quad (4)$$

where  $N_H$  is the number of hulls of size  $H$  and  $N_{tot}$  is the total number of hulls generated same as the number of clusters generated. Analogous to the form of the cluster size distribution function, the scaling function form of the hull size distribution is assumed, as

$$P_H(p) = H^{-\tau_H+1} f[H^{\sigma_H}(p - p_c)] \quad (5)$$

where  $\tau_H$  and  $\sigma_H$  are two exponents. The same scaling function form has already been verified for the spiral percolation hull[10].

Different moments of the hull size distribution  $P_H(p)$ ,  $\sum'_H H^k P_H(p)$  are expected to be singular as  $p \rightarrow p_c$ . The primed sum represents the sum of all finite hulls. The first, second and third moments  $\chi_H$ ,  $\chi'_H$  and  $\chi''_H$  of  $P_H(p)$  are calculated. The first moment  $\chi_H = \sum'_H H P_H(p)$  is the average hull size. The moments  $\chi_H$ ,  $\chi'_H$  and  $\chi''_H$  diverge with their respective critical exponents  $\gamma_H$ ,  $\delta_H$  and  $\eta_H$  at  $p = p_c$ . The critical exponents are defined as

$$\chi_H \sim |p - p_c|^{-\gamma_H}, \quad \chi'_H \sim |p - p_c|^{-\delta_H} \quad \& \quad \chi''_H \sim |p - p_c|^{-\eta_H}. \quad (6)$$

Since the hull related quantities are just different moments of the hull size distribution function  $P_H(p)$ , the critical exponents  $\gamma_H$ ,  $\delta_H$  and  $\eta_H$  then should be related to  $\tau_H$  and

$\sigma_H$ , exponents related to  $P_H(p)$ . It can be shown that the  $k$ th moment of the hull size distribution become singular as

$$\Sigma'_H H^k P_H(p) \sim (p - p_c)^{-(k - \tau_H + 2)/\sigma_H}. \quad (7)$$

The following scaling relations then can easily be obtained putting appropriate values of  $k$ , order of the moment of  $P_H(p)$ , in equation 7 and one obtains,

$$\gamma_H = (3 - \tau_H)/\sigma_H, \quad \delta_H = (4 - \tau_H)/\sigma_H \quad \& \quad \eta_H = (5 - \tau_H)/\sigma_H. \quad (8)$$

Eliminating  $\tau_H$  and  $\sigma_H$  from equation 8 a scaling relation can be obtained as

$$\eta_H = 2\delta_H - \gamma_H. \quad (9)$$

The exponents  $\tau_H$  and  $\sigma_H$  can also be estimated from the measured exponents  $\gamma_H$ ,  $\delta_H$  and  $\eta_H$  using the following relations

$$\begin{aligned} \tau_H &= (3\delta_H - 4\gamma_H)/(\delta_H - \gamma_H) = (4\eta_H - 5\delta_H)/(\eta_H - \delta_H) = (3\eta_H - 5\gamma_H)/(\eta_H - \gamma_H), \\ \sigma_H &= 1/(\delta_H - \gamma_H) = 1/(\eta_H - \delta_H) = 2/(\eta_H - \gamma_H). \end{aligned} \quad (10)$$

The values of the hull fractal dimension and other critical exponents will be estimated below and the scaling theory will be verified.

#### IV. RESULTS AND DISCUSSIONS

The critical properties of the DSP clusters have already been studied through Monte Carlo simulation and finite size scaling on both the square and triangular lattices [1, 2]. The values of the fractal dimension and other critical exponents of the cluster related quantities were estimated numerically and are listed in table I. The values of the critical exponents were found different from that of the other percolation models like OP, DP and SP and consequently the DSP model belongs to a new universality class[1]. It was observed that the spanning clusters are less anisotropic and more compact on the triangular lattice than those on the square lattice. This has happened due to the extra flexibility in the spiraling constraint on the triangular lattice. The change in the shape and compactness of the clusters had significant effect on the values of some of the critical exponents and fractal dimension. They were found considerably different on these two lattices for the DSP model and leads

to a breakdown of universality between the square and triangular lattices in  $2D$ [2]. Below, estimates of the hull fractal dimension and other critical exponents of the hull related quantities will be presented for anisotropic DSP cluster hulls for the first time. A comparison will be made between the results obtained on the square and triangular lattices, and also with that of the other percolation models.

To extract hulls, clusters are generated both on the square and triangular lattices at their percolation thresholds  $p_c \approx 0.655$  and  $0.570$  respectively. Different lattice sizes starting from  $L = 2^5$  to  $2^{11}$  have been used. Results are obtained through both single lattice ( $2^{11} \times 2^{11}$ ) Monte Carlo and finite size scaling methods. A total number  $N_{tot}$  of  $5 \times 10^4$  spanning clusters are generated for each lattice size  $L$  and every  $p$ , site occupation probability. Since each cluster has an associated hull, the number of hulls extracted are also  $N_{tot}$ . The size of the hull  $H$  is given by the number of occupied sites belonging to the hull.

The hull fractal dimension of the DSP clusters is determined following the scaling relation,  $H_\infty \sim L^{d_H}$ , equation 2. In Figure 4, average hull size of the spanning clusters  $H_\infty$  is plotted against the system size  $L$ . The squares represent the square lattice data and the triangles represent the triangular lattice data. The values of the hull dimension  $d_H$  are obtained as  $d_H = 1.458 \pm 0.008$  for the square lattice and  $d_H = 1.463 \pm 0.004$  for the triangular lattice. The hull fractal dimension  $d_H$  has also been measured by box counting method generating spanning clusters on the largest lattice ( $2^{11} \times 2^{11}$ ) considered here. The number of boxes occupied with a hull site  $N_B(\epsilon) \sim \epsilon^{d_H}$ , where  $\epsilon$  is the box size. The results are shown in the inset of Figure 4. The values of  $d_H$  obtained in the box counting method are given as  $1.44 \pm 0.01$  for the square and  $1.45 \pm 0.01$  for the triangular lattice. The errors quoted for both the methods are the least square fit errors taking into account the statistical error of each data point. The results obtained through box counting method and finite size scaling are within error bars. There are few things to notice. First, the hull fractal dimensions  $d_H$  measured on the square and triangular lattices in  $2D$  are found the same within error bars, approximately 1.46, whereas the cluster fractal dimension  $d_f$  were found different on the same lattices[2]. It could also be seen that, the hulls shown in Figure 2 and 3 of the clusters generated on the square and triangular lattices respectively are very identical on small length scales. However, DSP clusters are more compact and less anisotropic on the triangular lattice than on the square lattice. As a consequence, the cluster fractal dimension  $d_f$  and other critical exponents of the DSP clusters were found different on these two lattices

(see Table I). Thus, the extra flexibility given on the rotational constraint on the triangular lattice was only able to modify the critical behaviour of the whole cluster but unable to modify the critical properties of the external perimeter, the hull.

Second, the hull fractal dimension  $d_H$  obtained here is smaller than that of OP cluster hulls ( $7/4$ ). The OP cluster hulls generally contains long fjords or bays which are absent here. For OP cluster hulls, the value of  $d_H = 7/4$  was conjectured by Sapoval *et al* [8] through a relation  $d_H = 1 + 1/\nu$  connecting the hull dimension  $d_H$  and the connectivity length exponent  $\nu$  studying the diffusion fronts. (In the case of OP, the value of  $\nu$  is  $4/3$ ). This prediction was supported through large scale simulation by Ziff [13] and also proved analytically by Saleur and Duplantier [14]. It has already been observed that the conjecture does not hold true in the case of SP cluster hulls. The values of the connectivity exponents and hull fractal dimensions obtained for the SP clusters are:  $\nu(SP) \approx 1.116$  and  $d_H(SP) \approx 1.476$  ( $1 + 1/\nu \approx 1.896$ ) on the square lattice and  $\nu(SP) \approx 1.136$  and  $d_H(SP) \approx 1.466$  ( $1 + 1/\nu \approx 1.880$ ) on the triangular lattice [10]. Moreover, the DSP clusters are anisotropic and there are two connectivity length exponents  $\nu_{\parallel}$  and  $\nu_{\perp}$ . The hull dimension  $d_H$  here then may not be related to the connectivity length exponents  $\nu_{\parallel}$  and  $\nu_{\perp}$  of the anisotropic clusters in a simple manner as it was predicted by Sapoval *et al* for the case of isotropic clusters generated in OP. Interestingly, it is found that the hull dimension  $d_H$  calculated form the following relation

$$d_H = 1 + \frac{\nu_{\perp}}{\nu_{\parallel} + \nu_{\perp}} \quad (11)$$

is very close to the numerical values obtained here. Using equation 11, the hull dimensions  $d_H$  are obtained as  $d_H \approx 1.46$  on the square lattice and  $d_H \approx 1.47$  on the triangular lattice. It seems that for the anisotropic clusters generated in DSP, the hull dimension  $d_H$  is connected to the connectivity length exponents  $\nu_{\parallel}$  and  $\nu_{\perp}$  by the proposed relation in equation 11 and the relation proposed by Sapoval *et al* is valid only for the isotropic clusters generated in OP. However, an argument similar to the one given by Sapoval *et al*[8] would be possible only from the study of “anisotropic diffusion fronts”.

Third, the values of the hull fractal dimensions obtained for both the DSP and SP clusters are close to the fractal dimension  $D_e = 4/3$  of the externally accessible perimeter defined by Grossman and Aharony[15]. The external perimeter defined by Grossman and Aharony includes the sites available to a finite-size particle, coming from the outside, that is touching



the occupied sites on the cluster. This external perimeter excludes deep fjords or bays and consequently the fractal dimension found  $4/3$ . However, in the case of SP and DSP clusters, the hull is compact (or smooth) in comparison to the OP cluster hull due to the presence of rotational constraint in these models. The rotational constraint produces compact chiral dangling ends on the external boundary and makes the hull fractal dimension  $d_H$  closer to that of the Grossman-Aharony external perimeter. It should be mentioned here that similar value of hull fractal dimension close to  $4/3$  was also obtained numerically by Meakin and Family[16] and Rosso[17]. It was also observed experimentally in the study of invasion percolation fronts by Birovljev *et al*[18] and in the corrosion of thin Aluminum film by Balázs[19]. Deviation from the fractal dimension of  $7/4$  was also found in the study of self-stabilized etching of random systems by Sapoval *et al*[20]. Recently, Aizenman *et al* proved exactly the fractal dimension of Grossman-Aharony external perimeter is  $4/3$  [21].

The relation between the hull dimension  $d_H$  and the fractal dimension  $d_f$  of the percolation clusters is given by equation 3,  $H_\infty \sim S_\infty^x, x = d_H/d_f$ . This is verified here and the exponent  $x$  is calculated. In Figure 5, the average hull size  $H_\infty$  is plotted against the corresponding average size of the spanning clusters  $S_\infty$  for both the square and triangular lattices. The slope  $x = d_H/d_f$  is found as  $x = 0.839 \pm 0.006$  on the square lattice and  $x = 0.820 \pm 0.006$  on the triangular lattice. The errors are least square fit error taking into account the statistical error of each data point. The values of  $x$  are found close but only slightly different on the two lattices. This small difference in the value of  $x$  is consistent with the small difference in the cluster fractal dimensions  $d_f$  on the two lattices. The hull dimension  $d_H$  could be estimated from the relation  $d_H = x \times d_f$  and compared with the measured values. Taking the values of  $d_f$  from Ref.[1, 2], given in Table I, it is found that  $d_H = 1.45 \pm 0.01$  on the square lattice and  $d_H = 1.46 \pm 0.01$  on the triangular lattice which are within error bars of the measured value  $\approx 1.46$ . The errors quoted here are the propagation errors.

Now, the critical properties of different moments of the hull size distribution function are studied. The critical exponents related to the different moments of the hull size distribution  $P_H(p)$  are already defined in section III and the scaling relations are also described there. In this section, the values of the critical exponents are estimated and the scaling relations are verified. The first three moments  $\chi_H, \chi'_H$  and  $\chi''_H$  are plotted against  $|p - p_c|$  for the square lattice in Figure 6(a) and for the triangular lattice in Figure 6(b). The system size is taken

as  $L = 2048$ . The circles represent the average hull size  $\chi_H$ , the squares represent  $\chi'_H$ , the second moment and the triangles represent  $\chi''_H$ , the third moment in both the plots. The values of the exponents obtained are  $\gamma_H = 1.68 \pm 0.02$ ,  $\delta_H = 3.66 \pm 0.03$  and  $\eta_H = 5.70 \pm 0.05$  for the square lattice. For the triangular lattice, the values of the exponents obtained are  $\gamma_H = 1.71 \pm 0.02$ ,  $\delta_H = 3.69 \pm 0.03$  and  $\eta_H = 5.73 \pm 0.05$ . The errors quoted here are the standard least square fit error taking into account the statistical error of each single data point. The system size  $L$  dependence of the values of the critical exponents of different moments of the hull size distribution on the square and triangular lattices is also studied measuring the exponents' values at different  $L$ . The values of  $\gamma_H$ ,  $\delta_H$  and  $\eta_H$  are plotted against the inverse system size  $1/L$  in Figure 7(a), (b) and (c) respectively. The squares represent the square lattice data and the triangles represent the triangular lattice data in each plot. The values of the exponents obtained on these two lattices are converging to the values of the exponents obtained for  $L = 2048$  through MC simulation. The values of the hull moment exponents are also within the error bars on the square and triangular lattices. The hull fractal dimension  $d_H$  is already found the same on these two lattices. It should be mentioned here that the values of the critical exponents of the analogous cluster related quantities were found different on the square and triangular lattices [2]. Thus, breakdown of universality occurs in the cluster properties whereas universality holds for the associated hull properties in the DSP model in  $2D$  between the square and triangular lattices. This is a new observation and appears for the first time in a percolation model. The scaling relations could be verified now. The value of  $2\delta_H - \gamma_H = 5.64 \pm 0.08$  is very close to the value of the exponent  $\eta_H \approx 5.70$  for the square lattice. For the triangular lattice,  $2\delta_H - \gamma_H = 5.67 \pm 0.08$  and  $\eta_H \approx 5.73$ . The scaling relation  $\eta_H = 2\delta_H - \gamma_H$  (equation 9) is then valid within the error bars on both the lattices.

In table II, the values of the hull fractal dimension and other critical exponents are summarized and a comparison of the results obtained on the square and triangular lattices as well as on the SP model has been made. It can be seen that the universality holds for the hull results on the square and triangular lattice, as it is already mentioned, though there is a breakdown of universality for the cluster properties on the same lattices. It is interesting to note that the values of the exponents obtained here, especially the hull fractal dimension  $d_H$ , are very close to that of the SP (percolation under rotational constraint only) clusters hull[10] on both the lattices. However, the SP clusters were found much more compact than

the DSP clusters and are isotropic. The fractal dimension  $d_f$  of SP clusters on the square and triangular lattices are  $\approx 1.957$  and  $1.969$  respectively[10] whereas that of the DSP clusters are  $\approx 1.733$  [1] and  $1.775$  [2] respectively. It can be seen from the hull structures, given in Figure 2 and 3, that there exist chiral (clockwisely rotated) dangling ends on the perimeter as in the case of SP cluster hulls. The hull properties of both the DSP and SP clusters are then determined by the existence of chiral dangling ends on the external perimeter. These chiral dangling ends are generated due to the presence of the rotational constraint in both the models. The directional constraint then has a little effect on the hull critical properties and it is mostly determined by the rotational constraint present in the model. In a physical situation like transport of classical charged particles in disordered systems in the presence of crossed electric and magnetic fields, the magnetic properties then could be extracted from the external perimeter only whereas the electrical properties could be obtained from the bulk of the cluster.

Finally, the form of the hull size scaling function  $P_H(p) = H^{-\tau_H+1}f[H^{\sigma_H}(p-p_c)]$  is verified. The values of the exponents  $\tau_H$  and  $\sigma_H$  have been estimated using the scaling relation given in equation 10. For the square lattice, the estimates of  $\tau_H$  and  $\sigma_H$  are obtained as  $\tau_H = 2.17 \pm 0.02$  and  $\sigma_H = 0.498 \pm 0.003$ . These values are within the error bars of the values of  $\tau_H$  and  $\sigma_H$  obtained on the triangular lattice as  $\tau_H = 2.16 \pm 0.02$  and  $\sigma_H = 0.497 \pm 0.003$ . The errors mentioned correspond to propagation error only. The scaling function form is verified through data collapse by plotting  $P_H(p)/P_H(p_c)$  against the scaled variable  $H^{\sigma_H}(p - p_c)$  for both the square and triangular lattices in Figure 8(a) and (b), respectively. The hull size varies from 64 to 16384 and  $(p - p_c)$  is in the range 0.007 to  $-0.06$ . Not only a reasonable data collapse is observed for both the lattices but also the scaling function forms are found identical on the two lattices.

## V. CONCLUSION

Hulls of the DSP clusters are extracted generating large clusters at the percolation threshold and their properties are analyzed on both the square and triangular lattices in  $2D$ . Results are compared with that of other percolation models. The values of the hull fractal dimension  $d_H$  and critical exponents  $\gamma_H$ ,  $\delta_H$  and  $\eta_H$  related to the hull size distribution function  $P_H(p)$  are determined. It is found that the values obtained for the hull fractal di-

mension and the critical exponents related to the hull size distribution are the same within error bars on the square and triangular lattices unlike the cluster fractal dimension  $d_f$  and cluster related critical exponents of the DSP model. Thus, the universality of the hull critical exponents holds for the square and triangular lattices in  $2D$  whereas there is a breakdown of universality in the corresponding cluster properties. The value of  $d_H \approx 1.46$  obtained here is close to  $4/3$ , the fractal dimension of the Grossman-Aharony external perimeter and away from  $7/4$  proposed by Sapoval *et al* for the ordinary percolation hull. A new conjecture is made relating  $d_H$  and two connectivity length exponents  $\nu_{\parallel}$  and  $\nu_{\perp}$  for the anisotropic clusters. It is found that the values of  $d_H$  and other hull critical exponents are close to that of the SP cluster hulls. Hull critical properties are then mostly determined by the rotational constraint than the directional constraint present in the model. The critical exponents estimated here satisfy the scaling relations among themselves within error bars. The assumed scaling function form has been verified and found similar on both the square and triangular lattices.

## VI. ACKNOWLEDGMENT

The authors thank A. Srinivasan for helpful discussions. SS thanks CSIR, India for financial support.

- 
- [1] S. B. Santra, Eur. Phys. J. B **33**, 75 (2003); Int. J. Mod. Phys. B **17**, 5555 (2003).
  - [2] S. Sinha and S. B. Santra, Eur. Phys. J. B. **39**, 513 (2004).
  - [3] D. Stauffer and A. Aharony, *Introduction to Percolation Theory*, 2nd edition, (Taylor and Francis, London, 1994); A. Bunde and S. Havlin, in *Fractals and Disordered Systems*, edited by A. Bunde and S. Havlin (Springer-Verlag, Berlin, 1991).
  - [4] W. Kinzel, in *Percolation Structure and Processes*, edited by G. Deutscher, R. Zallen, and J. Adler (Adam Hilger, Bristol, 1983); H. Hinrichsen, Adv. Phys. **49**, 815 (2000).
  - [5] P. Ray and I. Bose, J. Phys. A **21**, 555 (1988); S. B. Santra and I. Bose, J. Phys. A **24**, 2367 (1991); J. Phys. A **25**, 1105 (1992). .
  - [6] R. A. Ramos, P. A. Rikvold, M. A. Novotny, Phys. Rev. B **59**, 9053 (1999); J. W. Evans, Rev.

- Mod. Phys. **65**, 1281 (1993).
- [7] S. B. Santra, B. Sapoval, Physics A **266**, 160 (1999); S. B. Santra, B. Sapoval, Ph. Barboux and F. Devreux, C. R. Acad. Sci. (Paris) **326**, 129 (1998).
  - [8] B. Sapoval, M. Rosso and J. F. Gouyet, J. Phys. Lett. **46**, L149 (1985); B. Sapoval, M. Rosso, J. F. Gouyet and J. F. Colonna, Solid State Ionics **18**, 21 (1986); M. Rosso, J. F. Gouyet and B. Sapoval, Phys. Rev. Lett **57**, 3195 (1986).
  - [9] R. F. Voss, J. Phys. A **17**, L373 (1984).
  - [10] S. B. Santra and I. Bose, J. Phys. A **26**, 3963 (1993)
  - [11] P. L. Leath, Phys Rev. B **14**, 5046 (1976).
  - [12] R. M. Ziff, P. T. Cummings and G. Stell, J. Phys. A **17** 3009 (1984)
  - [13] R. M. Ziff, Phys. Rev. Lett. **56**, 545 (1986)
  - [14] H. Saleur and B Duplantier, Phys. Rev. Lett. **58**, 2325 (1987)
  - [15] T. Grossman and A. Aharony, J. Phys. A **19**, L745 (1986); J. Phys. A **20**, L1193 (1987)
  - [16] P. Meakin and F. Family, Phys. Rev. A **34**, 2558 (1986).
  - [17] M. Rosso, J. Phys. A **22**, L131 (1989).
  - [18] A. Birovljev, L. Furuberg, J. Feder, T. Jssang, K. J. Mly and A. Aharony, Phys. Rev. Lett. **67**, 584 (1991).
  - [19] L. Balázs, Phys. Rev. E **54**, 1183 (1996).
  - [20] B. Sapoval, S. B. Santra and Ph. Barboux, Europhys. Lett. **41**, 297 (1998).
  - [21] M. Aizenman, B. Duplantier and A. Aharony, Phys. Rev. Lett. **83**, 1359 (1999)

Lattice Type	$d_f$	$\gamma$	$\delta$	$\eta$	$\nu_{\parallel}$	$\nu_{\perp}$	$\sigma$	$\tau$
Square[1]:	1.733	1.85	4.01	6.21	1.33	1.12	0.459	2.16
	$\pm 0.005$	$\pm 0.01$	$\pm 0.04$	$\pm 0.08$	$\pm 0.01$	$\pm 0.03$	$\pm 0.015$	$\pm 0.20$
	$1.72 \pm 0.02(\text{FS})$							
Triangular[2]:	1.775	1.98	4.30	6.66	1.36	1.23	0.427	2.16
	$\pm 0.004$	$\pm 0.02$	$\pm 0.04$	$\pm 0.08$	$\pm 0.02$	$\pm 0.02$	$\pm 0.003$	$\pm 0.02$
	$1.80 \pm 0.03(\text{FS})$							

TABLE I: Numerical estimates of the critical exponents and fractal dimension measured for the DSP clusters on the square and triangular lattices. Some of the critical exponents and the fractal dimension are significantly different on the two lattices.

Lattice Type	Model	$d_H$	$d_H^c$	$x$	$d_H = xd_f$	$\gamma_H$	$\delta_H$	$\eta_H$
Square	DSP	1.458	1.46	0.839	1.45	1.68	3.66	5.70
		$\pm 0.008$	$\pm 0.02$	$\pm 0.007$	$\pm 0.01$	$\pm 0.02$	$\pm 0.03$	$\pm 0.05$
		$d_H = 1.44 \pm 0.01$ (Box Counting)						
	SP	1.476		0.74		1.82	3.75	
		$\pm 0.005$		$\pm 0.02$		$\pm 0.01$	$\pm 0.02$	
Triangular	DSP	1.463	1.47	0.820	1.46	1.71	3.69	5.73
		$\pm 0.004$	$\pm 0.02$	$\pm 0.006$	$\pm 0.01$	$\pm 0.02$	$\pm 0.03$	$\pm 0.05$
		$d_H = 1.45 \pm 0.01$ (Box Counting)						
	SP	1.466		0.76		1.91	3.87	
		$\pm 0.016$		$\pm 0.02$		$\pm 0.01$	$\pm 0.03$	

TABLE II: Comparison of the hull exponents and hull fractal dimension measured for the DSP model on the square and triangular lattices as well as with that of the SP model.  $d_H^c$  is the hull fractal dimension obtained through the proposed conjecture:  $d_H = 1 + \nu_{\perp}/(\nu_{\parallel} + \nu_{\perp})$ .  $d_H$  is also measured from the relation  $d_H = xd_f$  considering the values of  $d_f$  as 1.733 and 1.775 (table I) for the square and triangular lattices respectively. Measurements are found consistent in different methods adopted. The exponents are almost same within the error bars on the two lattices. The hull fractal dimension in the DSP model is found within error bar of that of the SP model.

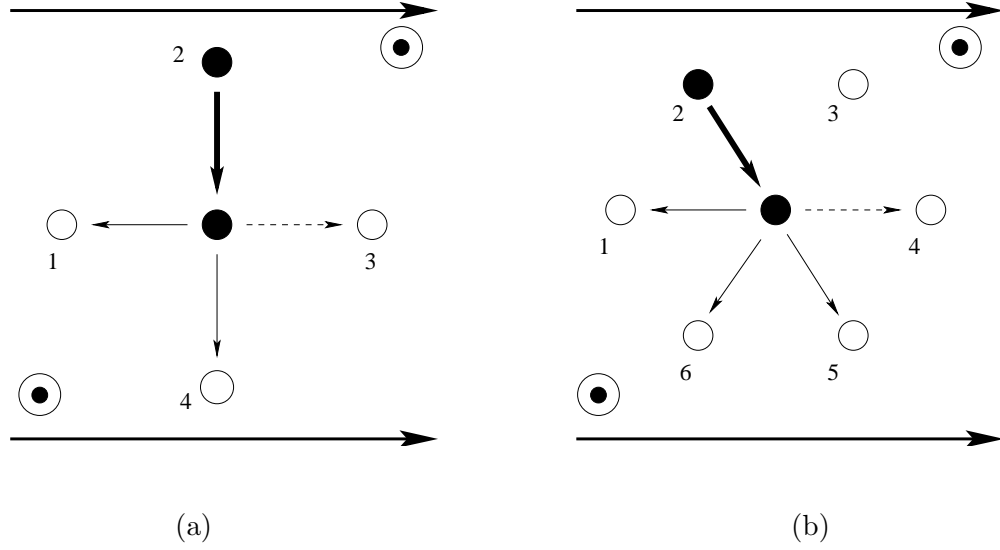


FIG. 1: Selection of empty nearest neighbours for occupation in a MC time step is demonstrated here on the square (a) and triangular (b) lattices. Black circles are the occupied sites and the open circles are the empty sites at a given time. Thick long arrows from left to right represent the directional constraint. The presence of clockwise rotational constraint is shown by encircled dots. The central site is occupied from site 2 and shown by short thick arrows. On the square lattice, site 3 on the right is always eligible for occupation due to the directional constraint, marked by dotted arrow and sites 4 and 1 are eligible for occupation due to the rotational constraint, marked by thin arrows. Similarly on the triangular lattice, site 4 due to the directional constraint and sites 5, 6 and 1 due to the rotational constraint are eligible for occupation.

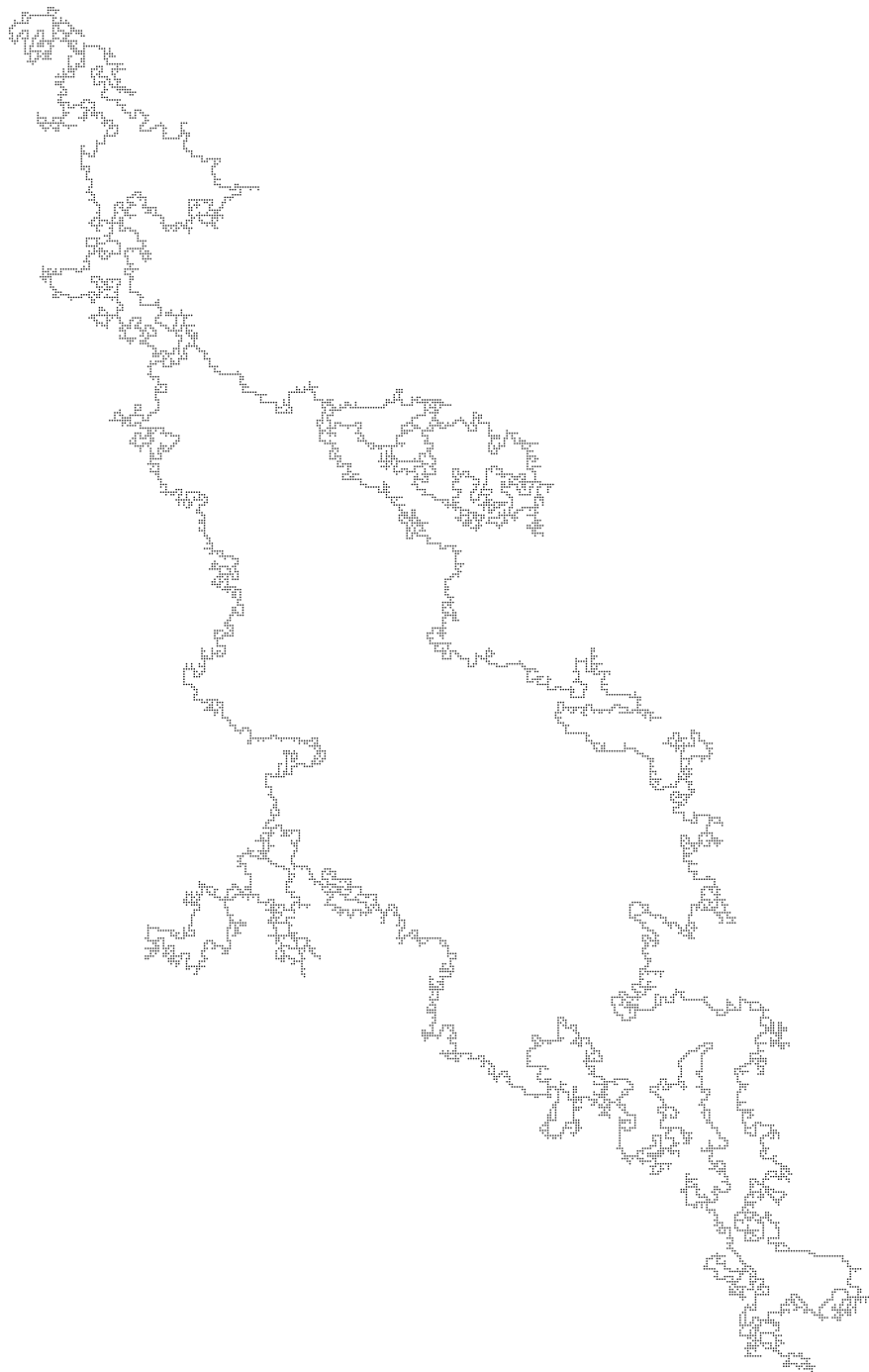


FIG. 2: Hull of a spanning cluster of size  $S = 23964$  on a  $256 \times 256$  square lattice at the percolation threshold  $p_c = 0.655$ . The size of the hull is  $H = 7938$ . It could be seen that the dangling ends are clockwise rotated and the cluster is anisotropic.



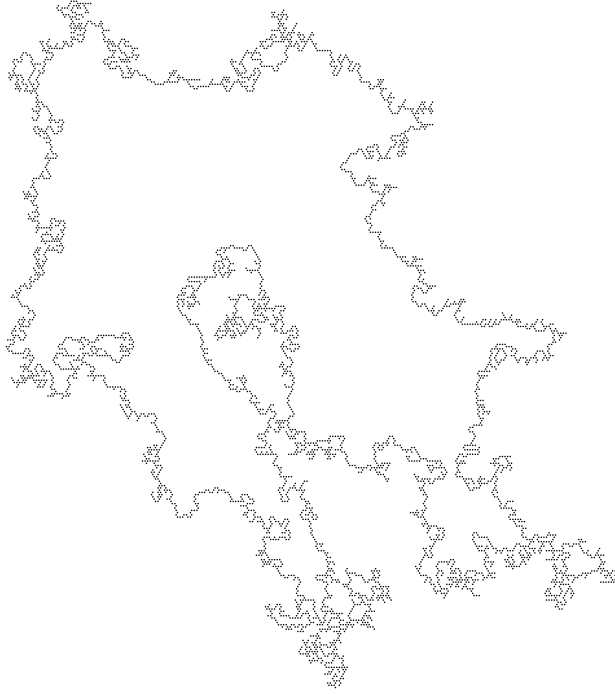


FIG. 3: Hull of a spanning cluster of size  $S = 15648$  on a  $256 \times 256$  triangular lattice at the percolation threshold  $p_c = 0.570$ . The size of the hull is  $H = 4370$ . There are chiral dangling ends but the cluster is less anisotropic than the cluster on the square lattice.

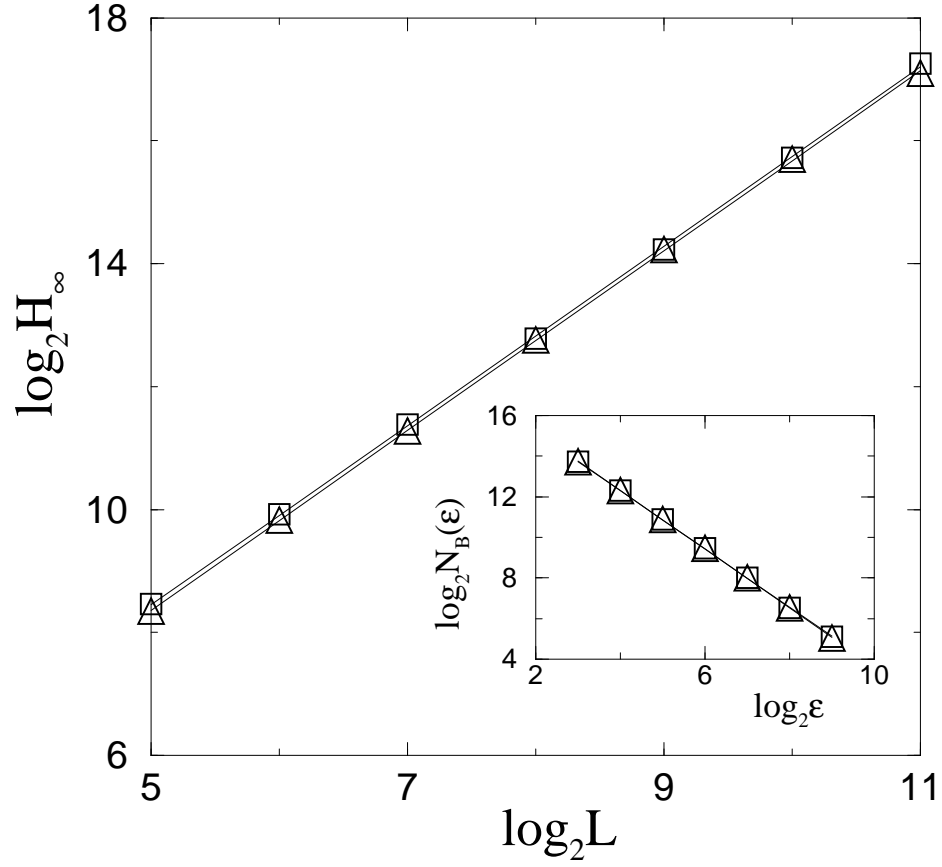


FIG. 4: Average hull size  $H_\infty$  of the spanning clusters versus the system size  $L$ . The squares represent the square lattice data and the triangles represent the triangular lattice data. The hull fractal dimensions are obtained as  $d_H = 1.458 \pm 0.008$  for the square lattice and  $1.463 \pm 0.004$  for the triangular lattice. In the inset, the number of boxes  $N_B(\epsilon)$  is plotted against the box size  $\epsilon$ . The hull fractal dimensions obtained by box counting method are  $d_H = 1.44 \pm 0.01$  for the square lattice and  $1.45 \pm 0.01$  for the triangular lattice. The values obtained in two different methods are within error bars. The value of  $d_H$  is also within error bars on the two lattices.

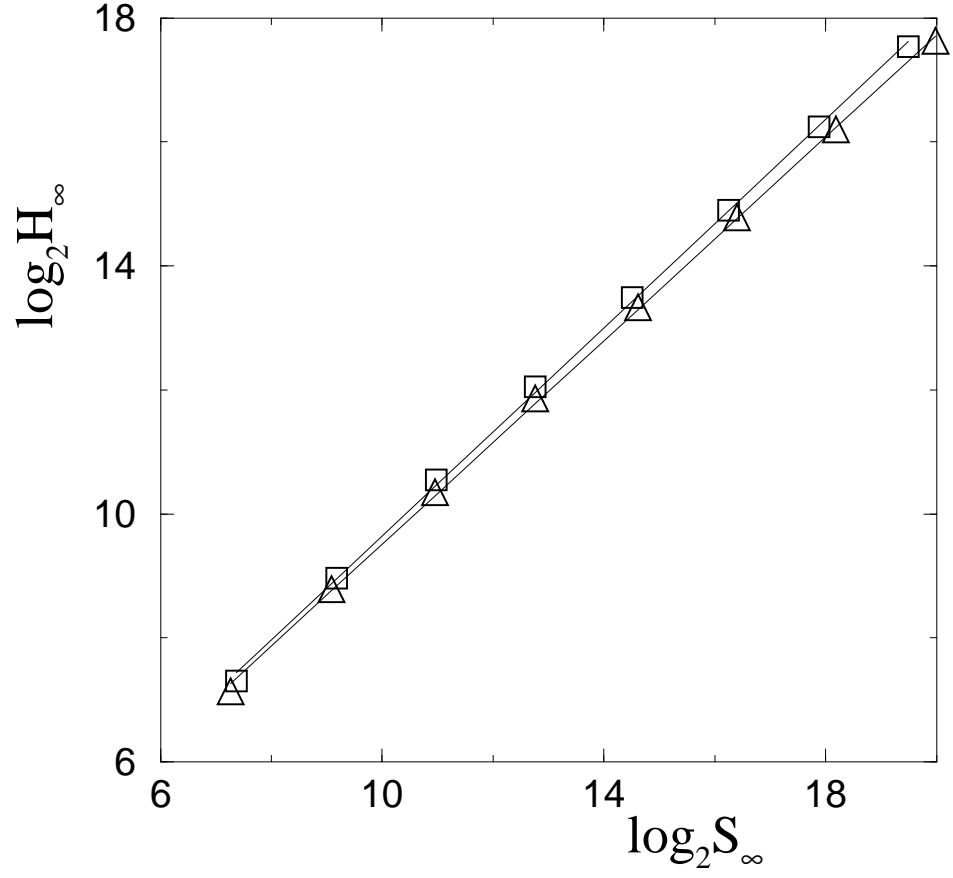


FIG. 5: Plot of average hull size  $H_\infty$  versus corresponding average cluster size  $S_\infty$  of the spanning clusters. The squares represent the square lattice data and the triangles represent the triangular lattice data. The values of the exponent  $x$  are obtained as  $x = 0.839 \pm 0.007$  for the square lattice and  $x = 0.820 \pm 0.006$  for the triangular lattice.

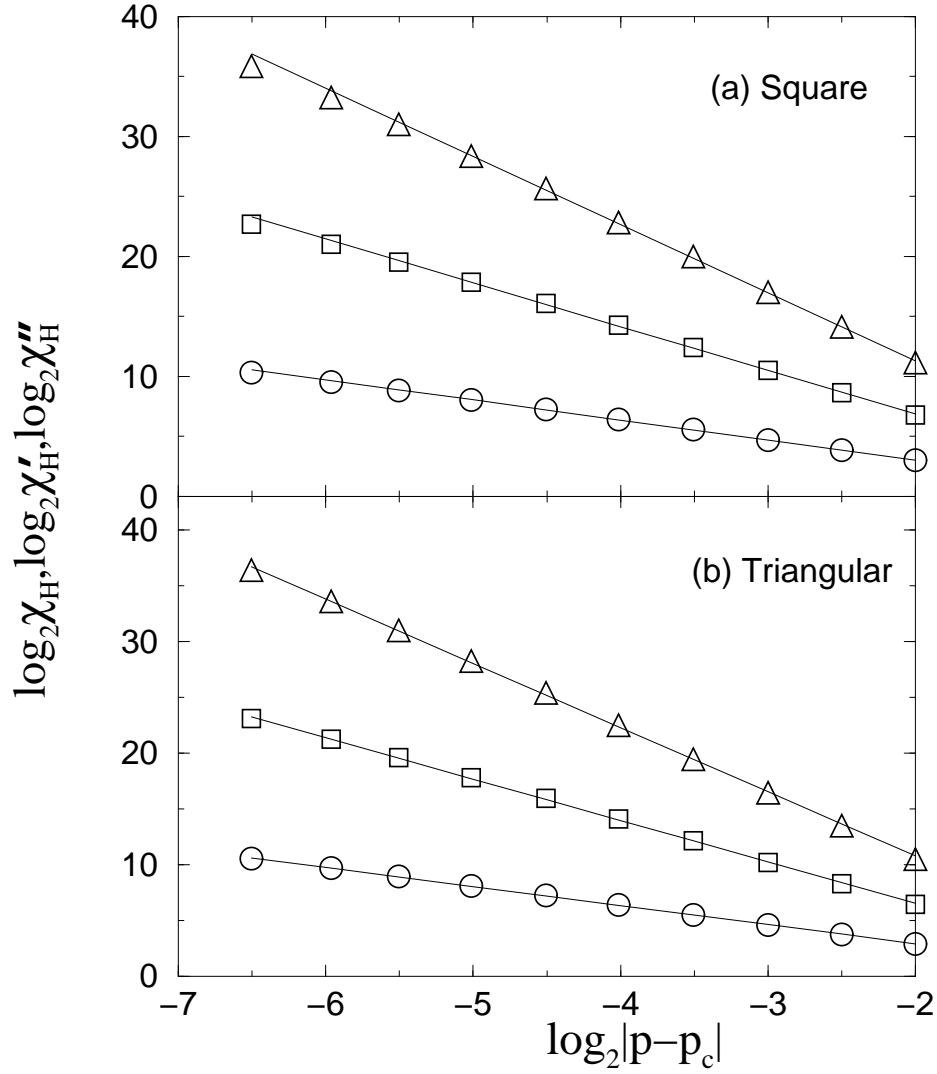


FIG. 6: Plot of the first, second and third moments  $\chi_H$ ,  $\chi'_H$  and  $\chi''_H$  of hull size distribution versus  $|p - p_c|$  for the lattice size  $L = 2048$  on the square (a) and triangular (b) lattices. Different symbols are circles for  $\chi_H$ , squares for  $\chi'_H$  and triangles for  $\chi''_H$  for each lattice. The solid lines represent the best fitted straight lines through the data points. The corresponding critical exponents are found as  $\gamma_H = 1.68 \pm 0.02$ ,  $\delta_H = 3.66 \pm 0.03$  and  $\eta_H = 5.70 \pm 0.05$  for the square lattice and  $\gamma_H = 1.71 \pm 0.02$ ,  $\delta_H = 3.69 \pm 0.03$  and  $\eta_H = 5.73 \pm 0.05$  for the triangular lattice.

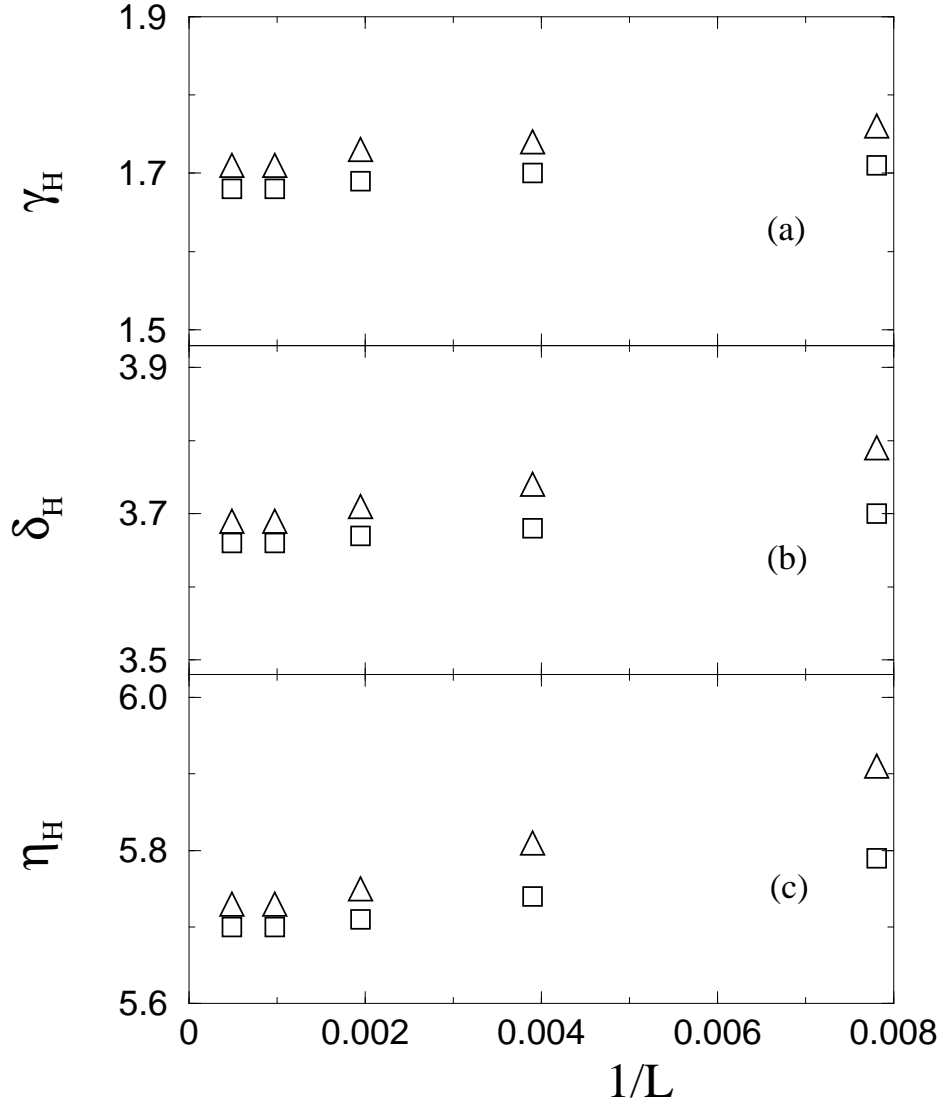


FIG. 7: Plot of the hull moments exponents  $\gamma_H$  (a),  $\delta_H$  (b) and  $\eta_H$  (c) against the inverse system size  $1/L$ . The system sizes considered are:  $L = 128, 256, 512, 1024$  and  $2048$ . The squares represent square lattice data and the triangles represent triangular lattice data. As  $L \rightarrow \infty$ , the exponents are converging to the values corresponding to  $L = 2048$ . The values of the exponents are within the error bar on the two lattices.

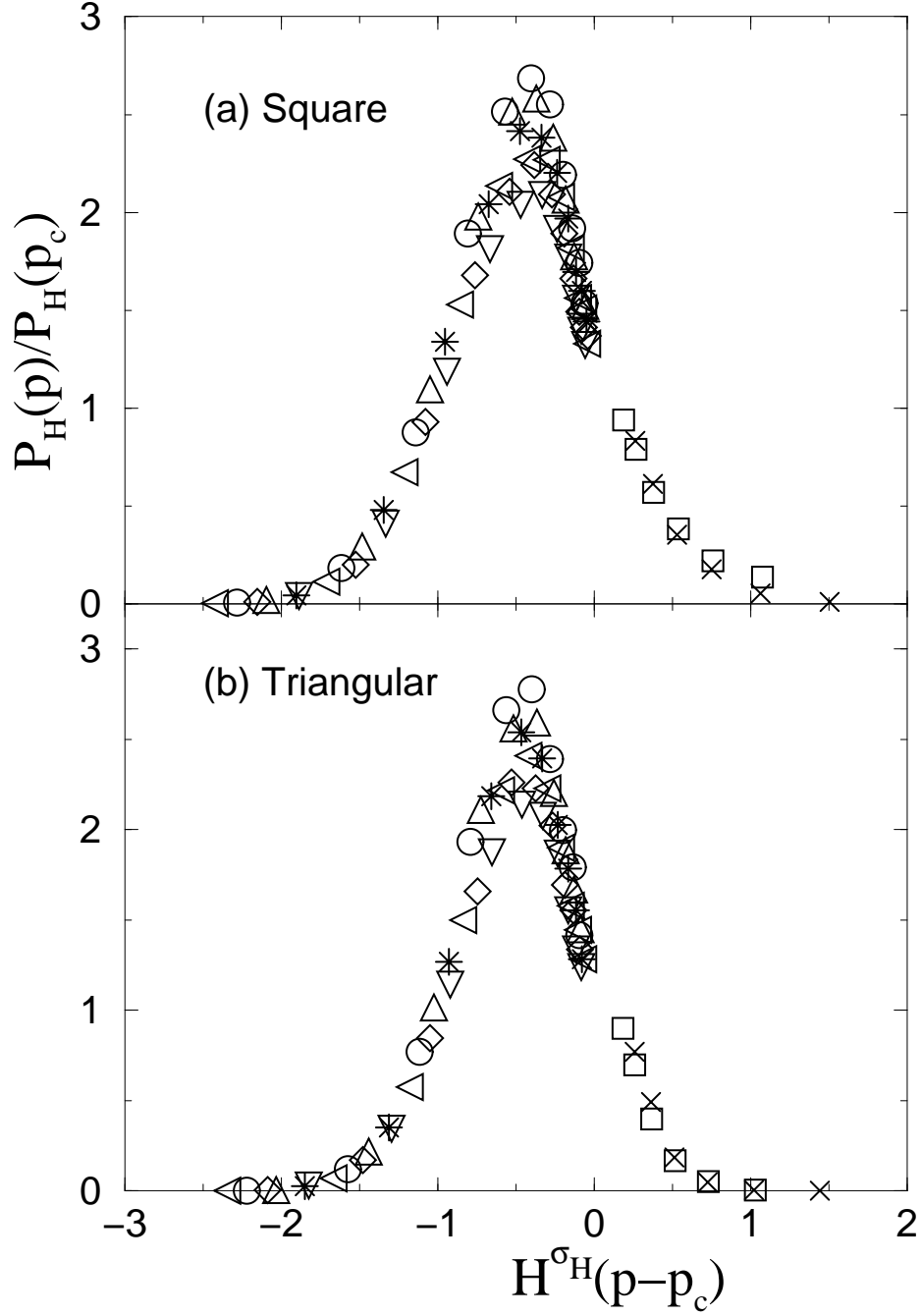


FIG. 8: Plot of scaled hull size distribution  $P_H(p)/P_H(p_c)$  versus scaled variable  $H^{\sigma_H}(p-p_c)$  for different values of  $p$  on the square (a) and triangular (b) lattices. The value of  $\sigma_H$  is taken as  $\sigma_H = 0.498$  (square) and  $\sigma_H = 0.497$  (triangular). The hull size  $H$  changes from 64 to 16384. The data plotted correspond to  $p-p_c = 0.007(\times)$ ,  $0.005(\square)$ ,  $-0.035(\nabla)$ ,  $-0.04(\diamond)$ ,  $-0.045(\triangleleft)$ ,  $-0.05(*)$ ,  $-0.055(\triangle)$ ,  $-0.06(\bigcirc)$  for both the plots. Reasonable data collapse are observed on both the lattices. Since the value  $\sigma_H$  is almost the same, the scaling function form looks almost identical on the two lattices.